GD2 ganglioside specific antibody treatment downregulates PI3K/Akt/mTOR signaling network in human neuroblastoma cell lines

MAŁGORZATA DURBAS*, IRENA HORWACIK*, ELŻBIETA BORATYN, ELŻBIETA KAMYCKA and HANNA ROKITA

Laboratory of Molecular Genetics and Virology, Faculty of Biochemistry, Biophysics and Biotechnology, Jagiellonian University, 30-387 Kraków, Poland

Received May 4, 2015; Accepted June 3, 2015

DOI: 10.3892/ijo.2015.3070

Abstract. Mechanisms leading to inhibitory effects of an anti-GD2 ganglioside (GD2) 14G2a mouse monoclonal antibody (mAb) and PI3K/Akt/mTOR pathway inhibitors on human neuroblastoma cell survival were studied *in vitro*. We have recently shown on IMR-32, CHP-134, and LA-N-1 neuroblastoma cells that targeting GD2 with the mAb decreases cell viability of the cell lines. In this study we used cytotoxicity assays, proteomic arrays and immunoblotting to evaluate the response of the three cell lines to the anti-GD2 14G2a mAb and specific PI3K/Akt/mTOR pathway inhibitors. We show here that the mAb modulates intracellular signal transduction through changes in several kinases and their substrates phosphorylation. More detailed analysis of the PI3K/Akt/mTOR pathway showed significant decrease in activity of Akt, mTOR, p70 S6 and 4E-BP1 proteins and transient increase in PTEN (a suppressor of the pathway), leading to inhibition of the signaling network responsible for stimulation of translation and proliferation. Additionally, combining the GD2-specific 14G2a mAb with an Akt inhibitor (perifosine), dual mTOR/PI3K inhibitors (BEZ-235 and SAR245409), and a pan-PI3K inhibitor (LY294002) was shown to enhance cytotoxic effects against IMR-32, CHP-134 and LA-N-1 cells. Our study extends knowledge on mechanisms of action of the 14G2a mAb on the neuroblastoma cells. Also, it stresses the need for further delineation of molecular signal orchestration aimed at more reasonable selection of drugs to target key cellular pathways in quest for better cure for neuroblastoma patients.

Correspondence to: Professor Hanna Rokita, Faculty of Biochemistry, Biophysics and Biotechnology, Jagiellonian University, 7 Gronostajowa St., 30-387 Kraków, Poland
E-mail: hanna.rokita@uj.edu.pl

*Contributed equally

Key words: neuroblastoma, GD2 ganglioside, monoclonal antibody, PI3K/Akt/mTOR pathway inhibitor, cancer

Introduction

High expression of surface GD2 ganglioside, *MYCN* gene amplification and aberrant activation of the PI3K pathway are major hallmarks of high risk neuroblastoma (1,2). GD2 ganglioside-targeted therapies using monoclonal antibodies are studied in phase III clinical trials for neuroblastoma patients. The mAbs can inhibit tumor growth by means of antibody-dependent cellular cytotoxicity (ADCC), complement-dependent cytotoxicity (CDC) and generation of the anti-idiotypic network (3,4). Moreover, the mAb therapies supplemented with additional agents, like GM-CSF, IL-2 or retinoic acid are now accepted as a standard treatment of high risk patients (5).

Several studies have evidenced that GD2-specific antibodies inhibit tumor growth without involvement of the immune system (6-8). The mechanisms of the anti-proliferative effects of the antibodies are only partially elucidated. In small cell lung cancer cell cultures anti-GD2 ganglioside monoclonal antibodies induced apoptosis through reduction of the phosphorylation levels of focal adhesion kinase (FAK) and the activation of p38 (6) as well as activation of c-Jun N terminal kinase (JNK) (7). Moreover, the anti-GD2 ganglioside mAbs were very efficient in combination with anticancer drugs to exert enhanced cytotoxicity against the afore-mentioned cells (7). Our studies showed that the anti-GD2 14G2a mAb decreases survival of IMR-32 human neuroblastoma cells in a dose-dependent manner through induction of apoptosis and also exerts a synergistic effect with doxorubicin and topotecan in killing IMR-32 cells in culture (8). It was also recently shown by us that the same mAb inhibits IMR-32 and LA-N-1 human neuroblastoma cells survival *in vitro*, through significant decrease in expression of all three Aurora kinases and phosphorylation (9). Moreover, the Aurora A kinase binding partners: P53, PHLDA1 and MYCN, were either upregulated as in case of P53 and PHLDA1, or downregulated (MYCN) in the 14G2a mAb-treated IMR-32 and CHP-134 human neuroblastoma cells contributing to the observed decrease in cell viability (9). Finally, Cochonneau *et al*, demonstrated that an *O*-acetyl-GD2 ganglioside specific mAb treatment inhibited tumor growth of IMR-5 neuroblastoma cells *in vivo* in a

NOD/SCID mouse model in the absence of operating ADCC and CDC mechanisms (10).

The phosphoinositide 3-kinase (PI3K), Akt and mammalian target of rapamycin (mTOR) pathway is the most frequently altered pathway in human tumors appearing as a central oncogenic driver, fundamental to all cancer cells (11,12). The pathway is prominently activated by many growth factors that signal through receptor tyrosine kinases. PI3Ks are recruited to receptor kinases and stimulate the conversion of phosphatidylinositol-4,5-bisphosphate (PIP2) to phosphatidylinositol-3,4,5-triphosphate (PIP_3) that provides a docking site for Akt, which thereby becomes activated (13). The serine/threonine kinase Akt/PKB regulates multiple biological processes including cell survival, proliferation, growth and glycogen metabolism (13,14). The serine/threonine kinase mTOR functions as two distinct complexes in the PI3K signaling network (12,15). mTOR complex 2 (mTORC2) phosphorylates key residues to activate Akt and other kinases, thus regulating survival, metabolism and the cytoskeleton. mTORC1 is a central regulator of cellular metabolism and biosynthesis, promoting anabolic processes such as ribosome biogenesis, translation and the synthesis of lipids and nucleotides while suppressing catabolic processes such as autophagy and lysosome biogenesis (15).

Inhibition of the PI3K/Akt/mTOR pathway has been the subject of extensive efforts. Numerous inhibitors have been developed that target almost every step of the pathway. Most of these compounds are either in preclinical development, or in clinical trials (13,16,17). These include ATP-competitive, dual inhibitors of class I PI3K and mTORC1/2, 'pan-PI3K' inhibitors, which inhibit all four isoforms of class I PI3K (α, β, δ and γ), isoform-specific inhibitors of the various PI3Ks, allosteric and catalytic inhibitors of Akt and ATP-competitive inhibitors of mTOR only.

Based on the vast amount of scientific data, it becomes clear that the clinical application of single inhibitors targeting only e.g., the PI3K/AKT/mTOR pathway shows limited activity. Blockage of the pathway usually does not induce cancer cell death, due to selection of compensatory pathways that maintain survival and restore tumor growth (12). Therefore, combinations of agents targeting multiple elements of various signaling networks may be important for treatment of cancer patients.

The findings prompted us to investigate effects of the 14G2a mAb on protein members of the PI3K/Akt/mTOR network in neuroblastoma cells *in vitro*. There are numerous elements of the pathway which have been downregulated upon the mAb addition, including Akt, mTOR, p70 S6 and AMPK kinases. We observed transient increase in PTEN, a suppressor of the pathway. Additionally, four different PI3K/Akt/mTOR pathway inhibitors (LY294002, perifosine, BEZ-235 and SAR245409) were used in combination with the monoclonal antibody to determine neuroblastoma cell viability. We showed that BEZ-235 was the most potent of the four drugs tested.

Materials and methods

Cell culture. Three GD2-positive human neuroblastoma cell lines were used in experiments, i.e., IMR-32 (ATCC, USA, CCL-127), LA-N-1 (ECACC, UK, 06041201) and CHP-134 (ECACC, 06122002). No research involving human subjects is reported. IMR-32 cells were grown in EMEM medium with addition of 10% fetal calf serum, 1% non-essential amino acid solution, 1 mM sodium pyruvate and 50 μg/ml gentamicin. LA-N-1 cells were grown in EMEM/F-12 (1:1) medium with 10% fetal calf serum, 1% non-essential amino acid solution, and 50 μg/ml gentamicin. CHP-134 cells were grown in RPMI-1640 medium with 10% fetal calf serum and 50 μg/ml gentamicin. All cell lines were cultured at 37˚C in a 5% CO_2 atmosphere and were routinely tested for mycoplasma contamination and were found negative (Lonza, USA).

Antibody purification. Two mouse monoclonal antibodies, i.e., 14G2a and PK136 were purified from hybridoma culture supernatants using the HiTrap Protein G HP column (GE Healthcare Bio-Sciences AB, Sweden) according to the manufacturer's protocol, dialyzed against PBS, and assayed for protein content using a BCA method (Sigma-Aldrich, Poland) (detailed in ref. 9). The hybridoma cell line producing the 14G2a mAb (IgG2a), binding to GD2, was provided by Dr R.A. Reisfeld (Scripps Institute, La Jolla, CA, USA) and the hybridoma cell line clone PK136 (a mouse isotype-matched control) was purchased from the ATCC, USA. The PK136 mAb recognizes an antigen expressed on murine NK cells isolated from some strains of mice (NK1.1) that is not expressed on non-lymphoid cells.

Antibody and drug treatment. Cells were incubated with the 14G2a mAb or PBS (control cells) at concentration of 40 μg/ml for 1 h at 4˚C and then seeded on 96-well plates ($2x10^4$ cells/100 μl/well for IMR-32, LA-N-1, and $0.5x10^4$ cells/100 μl/well for CHP-134, BD Falcon, Belgium) and incubated for 72 h. Concentration of the 14G2a mAb used in our *in vitro* model (40 μg/ml), can be reached in patients sera during immunotherapy. Despite the mAb side effects, clinical efficacy of the mAb in the treatment of neuroblastoma patients have been already reported (3). For viability tests, cellular ATP contents were measured (ATPlite - luminescence ATP detection assay system, Perkin-Elmer, USA). For protein isolation cells were cultured in 6-well plates ($1x10^6$ cells in 5 ml of culture medium for IMR-32 and LA-N-1 cells, and $0.25x10^6$ cells in 5 ml of culture medium for CHP-134 cells) and treated for a given time with the 14G2a mAb or PBS, as described above.

In some experiments the inhibitors perifosine (KRX-0401, S1037, Selleck, Germany), BEZ-235 (NVP-BEZ235, S1009, Selleck), SAR245409 (XL765, S1523, Selleck) and LY294002 (#9901, Cell Signaling, Lab-JOT, Poland) were used on IMR-32, LA-N-1 and CHP-134 cells. Tested ranges of concentrations of the inhibitors were perifosine (1-20 μM), BEZ-235 (0.01-2 μM), SAR245409 (1-100 μM) and LY294002 (2.5-80 μM). Inhibitors were added to cell cultures for 72 h. Control cells were treated with equivalent volume of DMSO or water (solvents for the inhibitors). In some experiments, cells were first treated with 14G2a (40 μg/ml) (or PBS) for 1 h on ice, and then inhibitors or diluents were added.

RNA isolation and quantitative RT-PCR. Total RNA samples were isolated from IMR-32 cells using TRI Reagent® as described in the manufacturer's protocol (Molecular Research

Center, Inc., USA; detailed in ref. 9). Briefly, 1 μg of total RNA was reverse-transcribed using Oligo(dT)15 Primer (Invitrogen, Poland) and M-MLV reverse transcriptase (Invitrogen). cDNA was analyzed using real-time PCR (Rotor-Gene 3000 system, Corbett Life Science, Australia). A KAPA SYBR FAST qPCR Master Mix (Kapa Biosystems, USA) was used in reactions. For sample normalization, the amount of eukaryotic translation elongation factor 2 (eEF2) cDNA was measured. Following primers were used: P27 (5'-GAAGCGACCTGCAACCGAC GATT-3', 5'-CAGGCTTCTTGGGCGTCTGCTC-3'); eEF-2 (5'-GGTGCAGTGCATCATCGAGGAGTC-3', 5'-TCGCGG TACGAGACGACCGG-3'). Sample quantification was performed in triplicates using the ΔΔCt relative quantification method.

Protein extract isolation and proteome array analysis. The Proteome Profiler Antibody Array from R&D Systems (Human Phospho-Kinase Array kit, ARY003, UK) was applied to simultaneously detect relative levels of multiple phosphorylated proteins in a single sample. Ca 250 μg of proteins was used for each nitrocellulose membrane. The assay was performed according to the manufacturer's instructions. Chemiluminescence was detected with a Tecan Infinite M200 microplate reader and the positive signals were identified and quantified.

Whole cell extracts were prepared using the TRI Reagent® method or lysis buffer from the Human Phospho-Kinase Array kit (see above). Nuclear and cytoplasmic fractions were isolated with a method described by Suzuki *et al* (18).

Immunoblotting. Western blot analyses were performed as previously described (9). The first group of antibodies (Ab) was from Cell Signaling Technology (USA), i.e., phospho-Akt Pathway Antibody Sampler kit (#9916), mTOR Substrates Antibody Sampler kit (#9862), and AMPK and ACC Antibody Sampler kit (#9957). Dilutions of all antibodies were 1:1,000 for: anti-phospho-Akt (Ser473) Ab, #4060; anti-phospho-Akt (Thr308) Ab, #2965; anti-Akt (pan) Ab, #4691; anti-phospho-c-Raf (Ser259) Ab, #9421; anti-phospho-GSK-3β (Ser9) Ab, #9323; anti-phospho-PTEN (Ser380) Ab, #9551; anti-phospho-PDK1 (Ser241) Ab, #3438; anti-phospho-mTOR (Ser2448) Ab, #5536; anti-mTOR Ab, #2983; anti-phospho-p70 S6 kinase (Thr389) Ab, #9234; anti-phospho-p70 S6 kinase (Ser371) Ab, #9208; anti-phospho-4E-BP1 (Thr37/46) Ab, #2855; anti-phospho-AMPKα (Thr172) Ab, #2535; anti-AMPKα Ab, #2603; anti-AMPKβ1/2 Ab, #4150; anti-phospho-acetyl-CoA carboxylase (Ser79) Ab, #3661, anti-TBP Ab, #8515 and acetyl-CoA carboxylase Ab, #3676. The other antibodies were from Sigma, i.e., anti-GAPDH, G8795 (1:40,000). The following HRP-conjugated antibodies were used: anti-rabbit IgG antibodies (Cell Signaling), #7074 (1:2,000) or anti-mouse IgG antibodies (Sigma), A-9044 (1:40,000). Immunoreactive bands were visualized by an enhanced chemiluminescence method (Immobilon Western HRP Substrate, Millipore, Poland) according to the manufacturer's protocol and their intensity was quantified by densitometric scanning (Quest Spot Cutter, Quantity One Analysis software, Bio-Rad). Glyceraldehyde 3-phosphate dehydrogenase (GAPDH), or TATA-box binding protein (TBP) reference proteins were used for normalization of protein samples signals. In figures, levels of the protein expression in control samples were set as 1.

Flow cytometry analysis of the GD2 ganglioside content. FACS analyses were routinely used to measure contents of GD2 on neuroblastoma cells using the 14G2a mAb. Cells were incubated for 40 min at 4˚C with 1 μg of the 14G2a mAb or the PK136 mAb in 2% BSA/PBS and then the cells were washed with 2% FBS/PBS. The binding of antibodies was detected with mouse Ig-specific FITC-conjugated goat $F(ab')_2$ fragments using flow cytometry (BD™ LSR II with BD FACSDiva software, BD Biosciences). Prior to cell collection propidium iodide was added and populations of alive (propidium iodide-negative) cells were analyzed for GD2 content, based on the staining with the PK136 mAb (a negative control) and the 14G2a mAb.

Statistical analyses. Data in the graphs and Table II are presented as means ± SEM (a standard error of the mean). All experiments were repeated at least three times. We used one-way ANOVA with repeated measurements to test for statistically significant differences in means in experiments with more than two independent groups. IC_{40} values, i.e., concentrations of inhibitors causing decrease of cellular ATP contents to 40% of control cells (treated with appropriate diluents) were obtained from equations of regression curves applied to mean ATP assay results (of three to four independent experiments). Uncertainty of each IC_{40} value was calculated from the fit parameters of the given regression curve with application of the law of error propagation. We applied series of pairwise tests (t-test), comparing, e.g., means of control and treated cells with following p-values: $^{*}p<0.05$, $^{**}p<0.01$, $^{***}p<0.001$. Statistical analyses were performed with R software (R version 2.15.1 Patched) and Excel (Microsoft, USA).

Results

Key intracellular pathways are affected in the 14G2a-treated IMR-32 cells. The presence of GD2 ganglioside on the cell lines used in experiments was routinely tested by flow cytometry and similar results demonstrating high (ca 95%) GD2 ganglioside content were obtained (data not shown).

Quantitative proteome profiling performed on cellular extracts revealed significant temporal changes in phosphorylation of several intracellular proteins isolated from the 14G2a mAb-treated IMR-32 cells (Table I). It was shown that the Akt/mTOR pathway is affected by the 14G2a mAb added at 2, 4, 8 and 24 h to the cultured cell line. Some proteins became hyperphosphorylated early up to 4 h upon the 14G2a mAb treatment (β-catenin, MEK1/2, ERK1/2, STAT5a/b and AMPKα2), while others were phosphorylated only at 2 h (MSK1/2, JNKpan, AMPKα1 and p38α). Moreover, such proteins as Hck and Fyn were hyperphosphorylated later, with maximum at 8 h.

The PI3K/Akt/mTOR pathway has an important role in cell metabolism, growth, migration, survival and angiogenesis (16) and therefore changes of the network after the 14G2a mAb treatment were analyzed in detail. Besides this pathway, the other signaling routes were obviously affected upon targeting of GD2 with the mAb: β-catenin involved in Wnt signaling as the transcription co-activator (19), was hyperphosphorylated and therefore destabilized. This leads to inhibition of the canonical Wnt/β-catenin pathway. The

Table I. Changes in protein phosphorylation in anti-GD2 ganglioside 14G2a mAb-treated IMR-32 human neuroblastoma cells.

Protein name	Phosphorylation site[a]	2 h	4 h	8 h	24 h
β-catenin	-	209	153	70	47
MSK1/2	S376/S360	190	92	38	57
JNKpan	T183/Y185, T221/Y223	187	40	60	95
MEK1/2	S218/S222, S222/S226	184	123	31	89
STAT5a	Y699	177	194	57	70
AMPKα1	T174	176	78	37	72
p38α	T180/Y182	174	67	20	9
STAT5b	Y699	168	157	52	56
STAT5a/b	Y699	161	143	57	49
ERK1/2	T202/Y204, T185/Y187	159	231	30	29
AMPKα2	T172	154	138	38	74
STAT6	Y641	153	101	50	43
Fgr	Y412	141	77	37	29
GSK-3α/β	S21/S9	133	66	32	75
STAT3	Y705	130	104	37	45
Akt	S473	129	102	36	45
STAT2	Y689	127	108	47	80
HSP27	S78/S82	127	72	9	65
Lck	Y394	108	81	15	29
CREB	S133	105	92	37	54
FAK	Y397	105	91	35	30
Yes	Y426	103	114	37	47
Lyn	Y397	100	101	31	96
eNOS	S1177	98	51	58	76
c-Jun	S63	97	79	75	145
STAT1	Y701	97	37	93	54
Chk-2	T68	91	89	58	42
STAT4	Y693	91	48	70	63
RSK1/2	S221	83	46	69	47
mTOR	S2448	80	105	88	67
p27	T157	79	34	37	39
Hck	Y411	78	127	260	123
RSK1/2/3	S380	73	41	56	40
p70 S6	T421/S424	73	39	80	52
p53	S46	70	37	51	66
p27	T198	69	29	27	23
p70 S6	T229	68	47	80	44
Src	Y419	67	120	106	89
p53	S392	67	55	64	60
p53	S15	65	39	49	62
paxillin	Y118	64	49	41	50
Akt	T308	63	38	69	78
Fyn	Y420	61	108	177	105
PLCγ-1	Y783	61	36	48	51
Pyk2	Y402	57	47	40	32
p70 S6	T389	43	13	35	16

[a]Phosphorylation profiles of 46 kinases were created by quantifying the mean spot pixel densities on proteomic arrays at 2, 4, 8, and 24 h and expressed as percent of the control.

Table II. IC_{40} values calculated for single agent and combined treatment of neuroblastoma cell lines.

	IC_{40}[a] (inhibitor)	IC_{40}[a] (inhibitor + 14G2a)	Fold change
LY294002			
IMR-32	34.72 (±9.57)	4.12 (±2.66)	8.4
LA-N-1	26.51 (±5.09)	14.86 (±1.00)	1.8
CHP-134	13.98 (±2.77)	0.79 (±0.79)	17.8
Perifosine			
IMR-32	12.53 (±0.01)	8.248 (±2.09)	1.5
LA-N-1	11.12 (±1.00)	10.39 (±0.34)	1.1
CHP-134	10.33 (±1.38)	4.32 (±0.12)	2.4
BEZ-235			
IMR-32	1.21 (±0.31)	0.17 (±0.06)	7.2
LA-N-1	0.18 (±0.26)	0.16 (±0.03)	1.2
CHP-134	0.16 (±0.03)	0.07 (±0.01)	2.4
SAR245409			
IMR-32	95.75 (±15.30)	73.34 (±2.41)	1.3
LA-N-1	93.75 (±17.23)	88.30 (±20.78)	1.1
CHP-134	85.67 (±2.72)	38.28 (±10.29)	2.2

[a]The IC_{40} values were calculated as the concentration of drugs (used alone or combined with the 14G2a mAb) that caused growth inhibition to 40% of controls treated with appropriated diluents.

mitogen-activated protein kinases (MAPKs), have been implicated in a variety of cellular processes such as proliferation, differentiation, motility, stress response, apoptosis and survival (20). The kinases include ERK1/2, JNK1-3 and p38, which became hyperphosphorylated early upon the mAb treatment (Table I) and next their phosphorylation was inhibited leading to decrease in their activity. Additionally, specific MAPK-activated protein kinases, known to amplify the MAPK signal, such as members of the RSK and MSK family were also initially hyper- and next hypo-phosphorylated upon the mAb addition (Table I). c-jun N-terminal kinase (JNK) is a kinase activated by cellular stress whereby leading to apoptosis (21). We have shown that at 2 h of incubation of IMR-32 cells with the 14G2a mAb, the kinase is activated at key amino acid residues by nearly doubled phosphorylation (Table I). The result is similar to other data on JNK activation by cisplatin in the anti-GD2 ganglioside mAb-treated small cell lung carcinoma (7). The protein is also activated by arsenium oxide in acute myelocytic leukemia, leading to cell death (22). One of mitogen-activated protein kinases (MAPK), p38α, known to respond to stress stimuli (23), becomes also activated in the 14G2a-treated IMR-32 cells at 2 h through increased phosphorylation exceeding the control >70% (Table I). Similar result was observed in small cell lung carcinoma treated with an anti-GD2 ganglioside antibody (6). Increase in p38α activity was also connected with loss of attachment to collagen type I in colon cancer cells and their cell death through anoikis (24).

The signal transducer and activator of transcription (STAT) family of transcription factors, known from their role in signaling pathways utilized by a large number of cytokines, growth factors and hormones (25), represented by STATs 1-6, was either early (STAT1 and STAT4), or late (STAT 2, 3, 5 and 6) dephosphorylated and therefore inhibited. Focal adhesion kinase (FAK), regulates cellular adhesion and apoptosis, therefore diminished phosphorylation at Tyr397 (Table I) resulting in increased detachment, decreased cell viability, and increased apoptosis (26). Based on the experiments we can conclude that the mAb affects several pivotal signaling routes that drive or influence the malignant phenotype of the cells.

Akt pathway is inhibited in the 14G2a-treated cells. Our proteomic analysis revealed profound inhibition of the pro-mitotic mTOR pathway upon the GD2 ganglioside-directed mAb addition through dephosphorylation of Akt, mTOR, and p70 S6 proteins that leads to decrease in their activities. The pathway appears to be important in neuroblastoma, therefore we have further characterized changes in levels and phosphorylation of the afore-mentioned proteins not only in IMR-32 cells but also in CHP-134 and LA-N-1 cells. Akt is activated through a dual phosphorylation mechanism at Thr308 located within its activation loop by PDK1 and at Ser473 by mTORC2. Activated Akt phosphorylates a large number of downstream targets such as mTOR and GSK-3 leading to either promotion of cell growth and G1 cell cycle progression, or promotion of glycogen metabolism and regulation of Wnt signaling, respectively (14).

Although Akt protein levels did not change greatly in the IMR-32 and CHP-134 cells treated with the mAb (Fig. 1A and D), its phosphorylation on key amino acid residues, Ser473 and Thr308, was statistically significantly and severely decreased in the IMR-32 cells (Fig. 1B and C) and to smaller extent in CHP-134, in which p-Thr308 was significantly lower only at 24 h (Fig. 1E and F). We have shown that the kinase is dephosphorylated at Thr308 already after 2 h of incubation of IMR-32 cells with the antibody, and next after 6, 24 and 48 h the effect is more evident reaching ca 20% of the control at 48 h (Fig. 1C), while in CHP-134 dephosphorylation is reaching only ca 80% of the control (Fig. 1F). Interestingly, phosphorylation of PKD1 itself at Ser241 has not been clearly changed (as shown in Fig. 3E), in agreement with our major conclusion on the pathway inhibition under the 14G2a mAb treatment. Dephosphorylation of Ser473 in Akt takes place in the IMR-32 cells at 2 h and after 48 h reaching only 20% of the control (Fig. 1B), while in the CHP-134 cells the lowest value constitutes ca 65% of the control (Fig. 1E), this result on IMR-32 is similar to our proteomic array in which we have also found significant dephosphorylation of Akt at 8 and 24 h (Table I). Dephosphorylation of Thr308 and Ser473 by the intracellular phosphatases, protein phosphatase 2 (PP2) and PH domain leucine-rich repeat protein phosphatase (PHLPP), respectively, terminates Akt signaling (14), and we found similar effect of the 14G2a mAb on the treated cells.

P27 is a negative regulator of cell cycle progression in G1-S phase through inhibition of cyclins E-Cdk2 and D-Cdk4 and cyclin-dependent kinases (27). Akt kinase is able to phosphorylate P27 at Thr157 and Thr198 leading to cytoplasmic

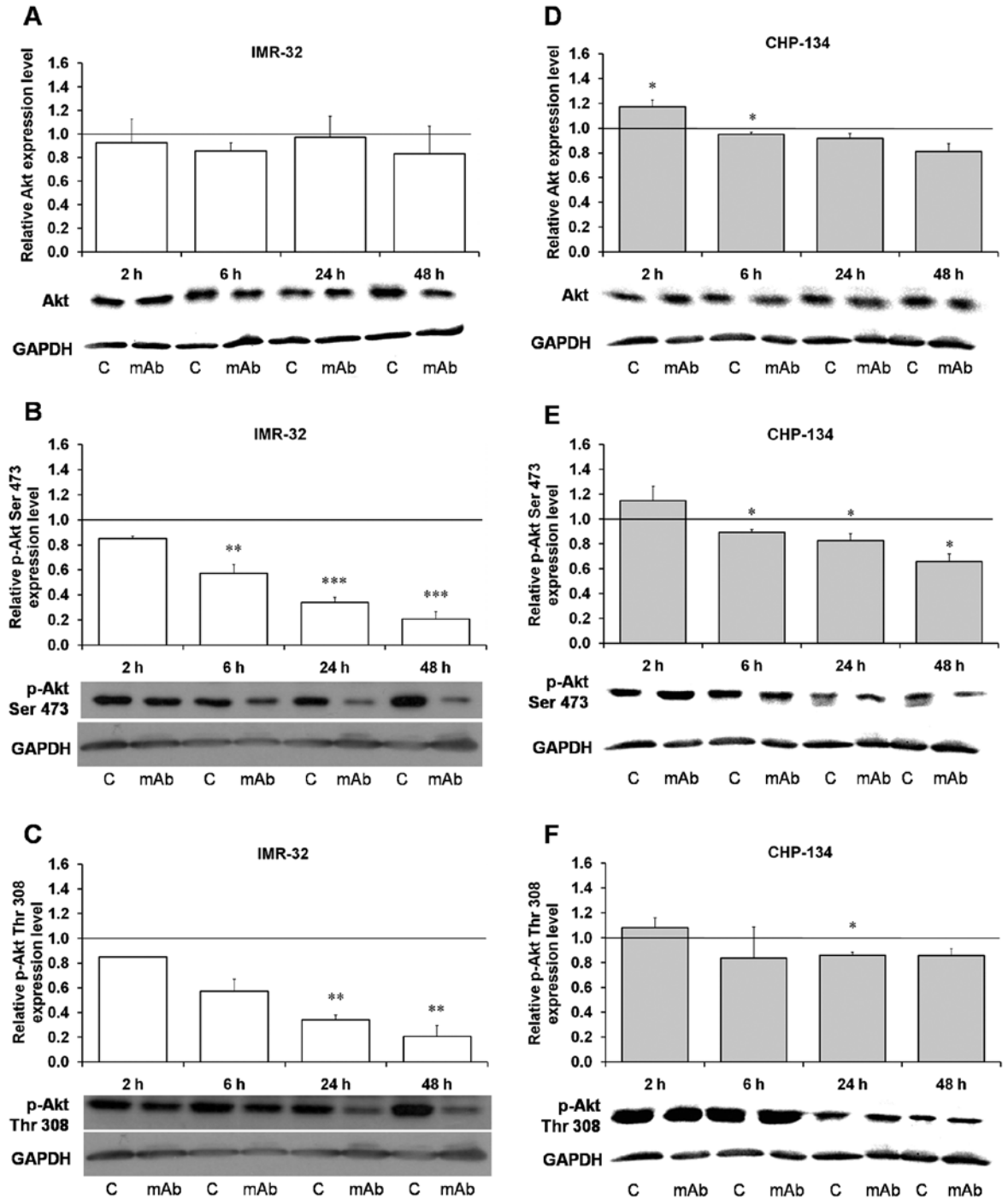

Figure 1. Effect of the 14G2a mAb on Akt expression and phosphorylation. Akt and phosphorylated Akt (p-Akt, Ser473 and Thr308) were measured at 2, 6, 24 and 48 h, and normalized to GAPDH. Mean values of three separate experiments obtained for the 14G2a mAb-treated IMR-32 (A-C) and CHP-134 (D-F) cells are presented (± SEM), and calculated versus control values, set as 1 (black baseline). ANOVA shows statistically significant changes of protein content in time in IMR-32 cells: p-Akt Ser473 [$F(3,8)=61.26$, $p<0.0001$], p-Akt Thr308 [$F(3,8)=12.08$, $p=0.0024$] and in CHP-134 cells: Akt [$F(3,9)=12.02$, $p=0.0017$], p-Akt Ser473 [$F(3,9)=8.50$, $p=0.0054$]. ANOVA shows no statistically significant changes of expression in time for the rest of the proteins. P-values for t-test were as follows: $^{*}p<0.05$, $^{**}p<0.01$, $^{***}p<0.001$. Below each chart representative immunoblottings are presented: C, control cells; mAb, mAb-treated cells (40 μg/ml).

retention of the protein (27,28). We found that P27 protein phosphorylation at both amino acids is inhibited as early as at 2 h in the 14G2a mAb-treated IMR-32 cells (Table I) and the effect is deepened up to 24 h. Q-RT-PCR revealed an early decrease and next at 48 h a return to a control level in *P27* mRNA content in the IMR-32 cells treated with the 14G2a mAb for 6-48 h (Fig. 2A). Moreover, the protein total cellular levels were increased in the IMR-32 and LA-N-1 cells although statistically significant increase was observed only in the IMR-32 cells at 24 and 48 h (Fig. 2B and C) probably due to increased transcript stability and/or efficient translation. Finally, analysis of P27 protein expression in cytoplasmic fraction of the IMR-32 cells shows decreased levels at 24 and 48 h (Fig. 2D) with concomitant increase in nuclear content (Fig. 2E), further supporting our conclusion of possible participation of P27 in cell cycle inhibition in the analyzed model.

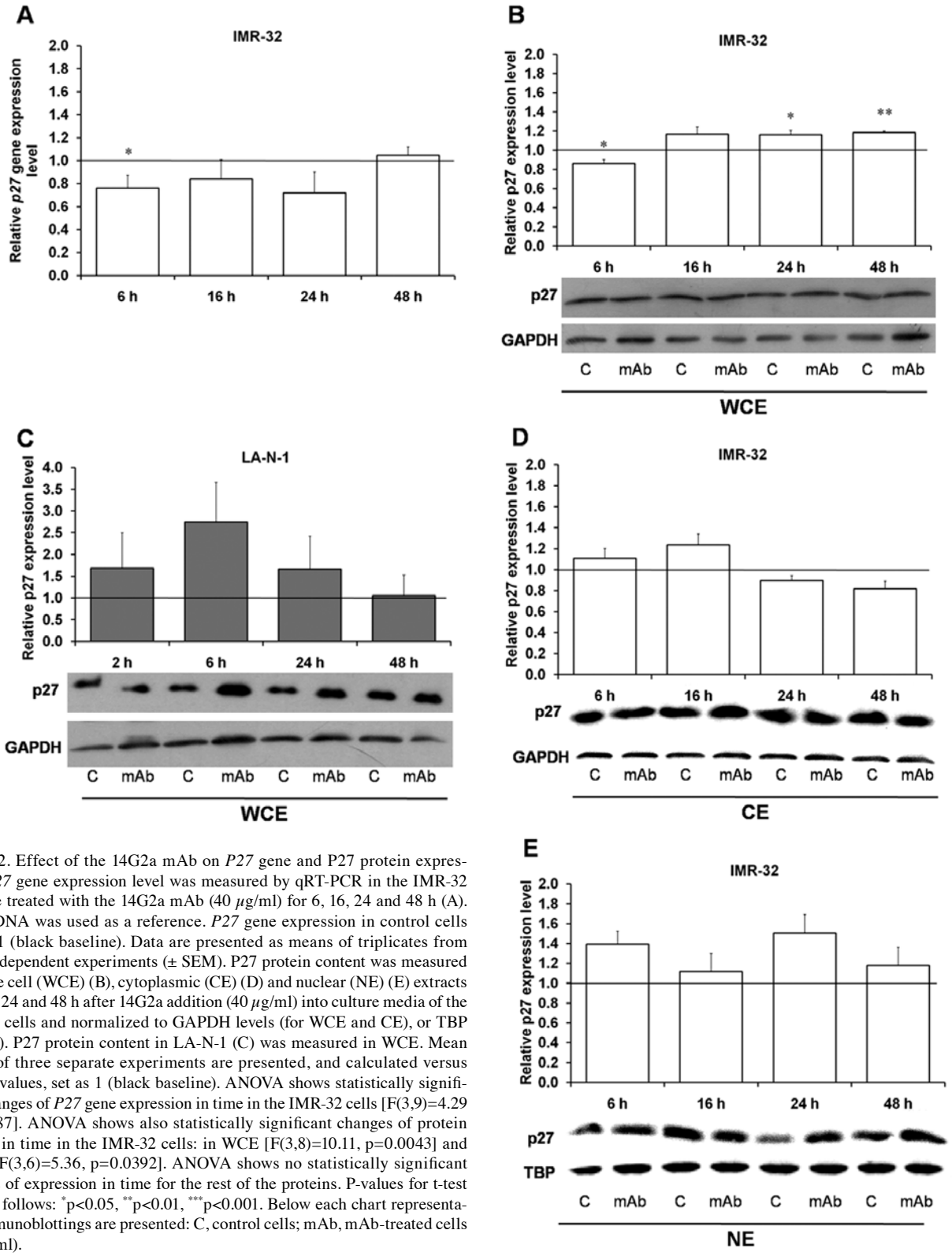

Figure 2. Effect of the 14G2a mAb on *P27* gene and P27 protein expression. *P27* gene expression level was measured by qRT-PCR in the IMR-32 cell line treated with the 14G2a mAb (40 μg/ml) for 6, 16, 24 and 48 h (A). EF-2 cDNA was used as a reference. *P27* gene expression in control cells equals 1 (black baseline). Data are presented as means of triplicates from three independent experiments (± SEM). P27 protein content was measured in whole cell (WCE) (B), cytoplasmic (CE) (D) and nuclear (NE) (E) extracts at 6, 16, 24 and 48 h after 14G2a addition (40 μg/ml) into culture media of the IMR-32 cells and normalized to GAPDH levels (for WCE and CE), or TBP (for NE). P27 protein content in LA-N-1 (C) was measured in WCE. Mean values of three separate experiments are presented, and calculated versus control values, set as 1 (black baseline). ANOVA shows statistically significant changes of *P27* gene expression in time in the IMR-32 cells [$F(3,9)=4.29$ $p=0.0387$]. ANOVA shows also statistically significant changes of protein content in time in the IMR-32 cells: in WCE [$F(3,8)=10.11$, $p=0.0043$] and in CE [$F(3,6)=5.36$, $p=0.0392$]. ANOVA shows no statistically significant changes of expression in time for the rest of the proteins. P-values for t-test were as follows: $^{*}p<0.05$, $^{**}p<0.01$, $^{***}p<0.001$. Below each chart representative immunoblottings are presented: C, control cells; mAb, mAb-treated cells (40 μg/ml).

Phosphatase and tensin homolog (PTEN), a lipid phosphatase (mostly for phosphatidylinositol-3,4,5-triphosphate - PIP_3) that catalyzes the dephosphorylation of PIP_3, is a major negative regulator of PI3K and Akt signaling (11). Thus, the phosphatase counteracts PI3K by degrading its product, PIP_3. *PTEN* gene inactivation can be responsible for aberrant activation of the PI3K signaling in prostate cancer (29,30). We have shown that neither in IMR-32, nor in CHP-134 cells, the PTEN phosphatase phosphorylation at Ser380 is statistically significantly changed upon the 14G2a mAb treatment except for an increase observed in the IMR-32 cells at 6 h (Fig. 3A and B). PTEN phosphorylation at Ser380 constitutes a mechanism of PTEN inactivation in gastric cancer (31), therefore we can conclude that in the mAb-treated human neuroblastoma cells

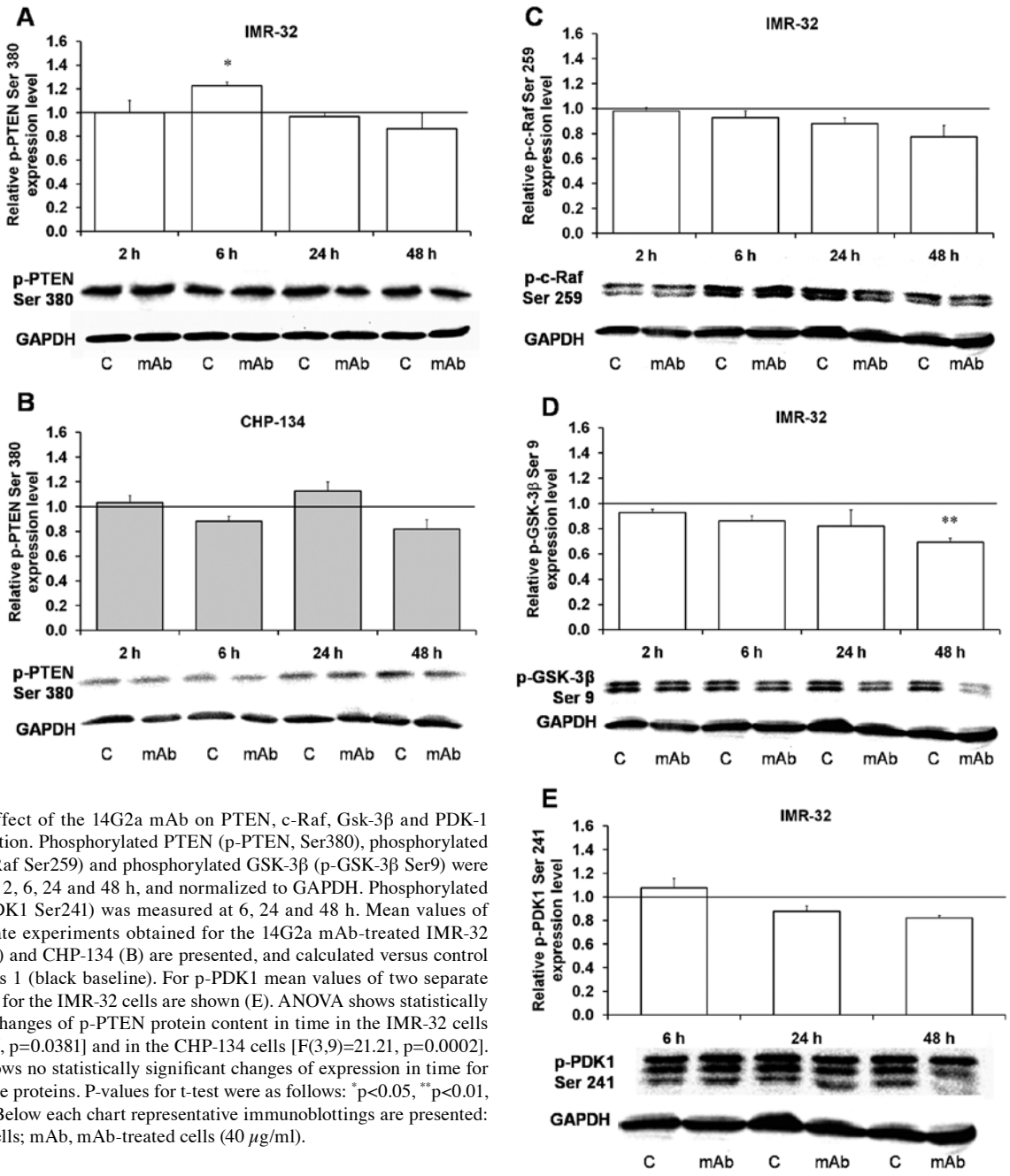

Figure 3. Effect of the 14G2a mAb on PTEN, c-Raf, Gsk-3β and PDK-1 phosphorylation. Phosphorylated PTEN (p-PTEN, Ser380), phosphorylated c-Raf (p-c-Raf Ser259) and phosphorylated GSK-3β (p-GSK-3β Ser9) were measured at 2, 6, 24 and 48 h, and normalized to GAPDH. Phosphorylated PDK1 (p-PDK1 Ser241) was measured at 6, 24 and 48 h. Mean values of three separate experiments obtained for the 14G2a mAb-treated IMR-32 (A, C and D) and CHP-134 (B) are presented, and calculated versus control values, set as 1 (black baseline). For p-PDK1 mean values of two separate experiments for the IMR-32 cells are shown (E). ANOVA shows statistically significant changes of p-PTEN protein content in time in the IMR-32 cells [$F(3,8)=4.57$, $p=0.0381$] and in the CHP-134 cells [$F(3,9)=21.21$, $p=0.0002$]. ANOVA shows no statistically significant changes of expression in time for the rest of the proteins. P-values for t-test were as follows: $^{*}p<0.05$, $^{**}p<0.01$, $^{***}p<0.001$. Below each chart representative immunoblottings are presented: C, control cells; mAb, mAb-treated cells (40 μg/ml).

used in the study, the phosphatase is still active. Additionally, we have shown that c-Raf, a member of MAPKKKs (32), is slightly dephosphorylated at Ser259 (an inhibitory site) in the IMR-32 cells (Fig. 3C). The reduction of the phosphorylation state of c-Raf at Ser259 is following the inhibition of Akt in PC3 cells (a human prostatic adenocarcinoma cell line) (32).

Akt regulates the storage of glucose in the form of glycogen by phosphorylating glycogen synthase kinase (GSK)-3β at Ser9 and -3α at Ser21, whereby blocking its kinase activity. Inhibitory phosphorylation of GSK-3β and 3α is not only promoting glycogen metabolism but also cell cycle progression and regulation of Wnt signaling (14). Significant inhibition of phosphorylation of GSK-3β at Ser9 found in the 14G2a mAb-treated IMR-32 cells (Table I and Fig. 3D) follows similar changes as the phosphorylated Akt and therefore can result in decreased proliferation of neuroblastoma cells.

mTOR pathway is inhibited in the 14G2a-treated cells. Activation of PI3K and Akt results in mTOR phosphorylation at Ser2448 (33), which next stimulates two major pathways leading to increased protein synthesis. The mTOR phosphorylates eukaryotic translation initiation factor 4E-binding protein 1 (4E-BP1), responsible for inhibition of eukaryotic translation initiation factor 4E (eIF-4E), which leads to release of 4E-BP1 and thus suppression of inhibition. The other pathway stimulated by mTOR involves activating phosphorylation of serine-threonine kinase 70S6 (p70 S6). The kinase phosphorylates proteins of ribosomal subunit 40S, causing recruitment of the subunit to active polysomes (34).

We found that in the 14G2a-treated IMR-32 cells, mTOR protein expression is decreased to ca 60% of the control, although in the CHP-134 and the LA-N-1 cells the decrease is smaller (Fig. 4A, C and E). However, mTOR phosphorylation

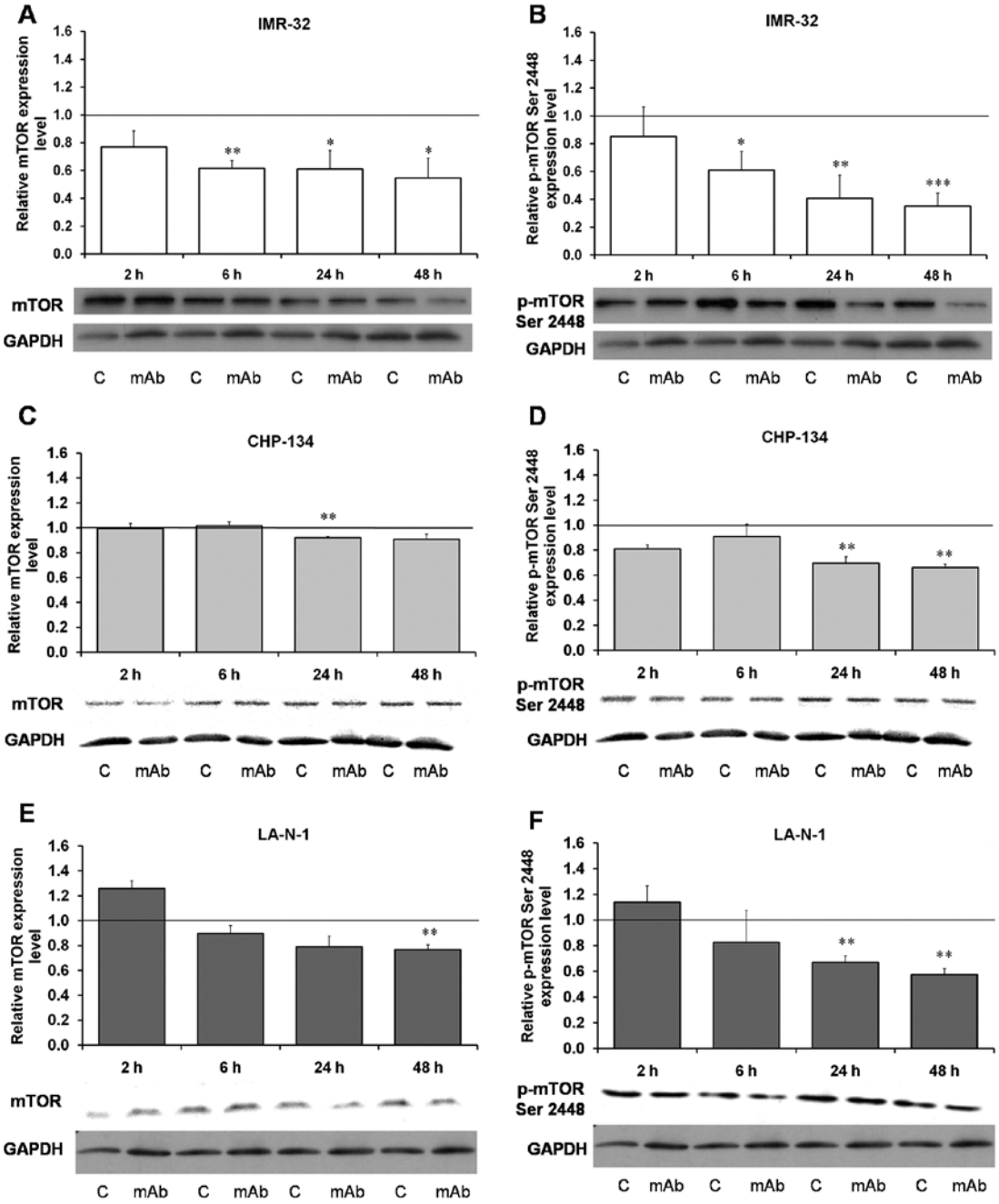

Figure 4. Effect of the 14G2a mAb on mTOR expression and phosphorylation. mTOR and phosphorylated mTOR (p-mTOR, Ser2448) were measured at 2, 6, 24 and 48 h, and normalized to GAPDH. Mean values of three or four separate experiments obtained for the 14G2a mAb-treated IMR-32 (A and B) and CHP-134 (C and D) and LA-N-1 cells (E and F) are presented, and calculated versus control values, set as 1 (black baseline). ANOVA shows statistically significant changes of mTOR content in time in the IMR-32 cells [$F(3,8)=42.15$, $p<0.0001$] and the LA-N-1 cells [$F(3,9)=4.01$, $p=0.0458$] and changes of p-mTOR content in time in the LA-N-1 cells [$F(3,9)=12.62$, $p=0.0014$]. ANOVA shows no statistically significant changes of expression in time for the rest of the proteins. P-values for t-test were as follows: $^{*}p<0.05$, $^{**}p<0.01$, $^{***}p<0.001$. Below each chart representative immunoblottings are presented: C, control cells; mAb, mAb-treated cells (40 μg/ml).

at Ser2448, responsible for its activity, decreases statistically significantly in all three cell lines, with the most pronounced inhibition in the IMR-32 cells at 48 h (Fig. 4B, D and F). The latter result was not so pronounced in our proteomic arrays, and only 33% inhibition of Ser2448 phosphorylation was observed in IMR-32 cells at 24 h (Table I).

P70 ribosomal S6 kinase (S6K1), a major substrate of the mTOR, exists as two protein isoforms, p85 and p70, because of the use of alternative ATG start codons. There are several phosphorylation sites in p70 S6 kinase, including Thr389 and Thr229, vital for its activity (35). Phosphorylation of Thr421 and Ser424 in autoinhibitory domain of the kinase is also contributing to its increased activity (36). In our studies, three sites of phosphorylation on kinase p70 S6 at Thr389, Thr229 and Thr421/Ser424 are characterized by early and significant decrease, especially at Thr389 in the IMR-32 cells treated with the mAb (Table I) and similar spectacular inhibition was observed in the same cell line and additionally in the LA-N-1 cells at Thr389 for 70 and 85 kDa isoforms of the enzyme (Fig. 5A, C, E and G). Phosphorylation at Ser371, indispens-

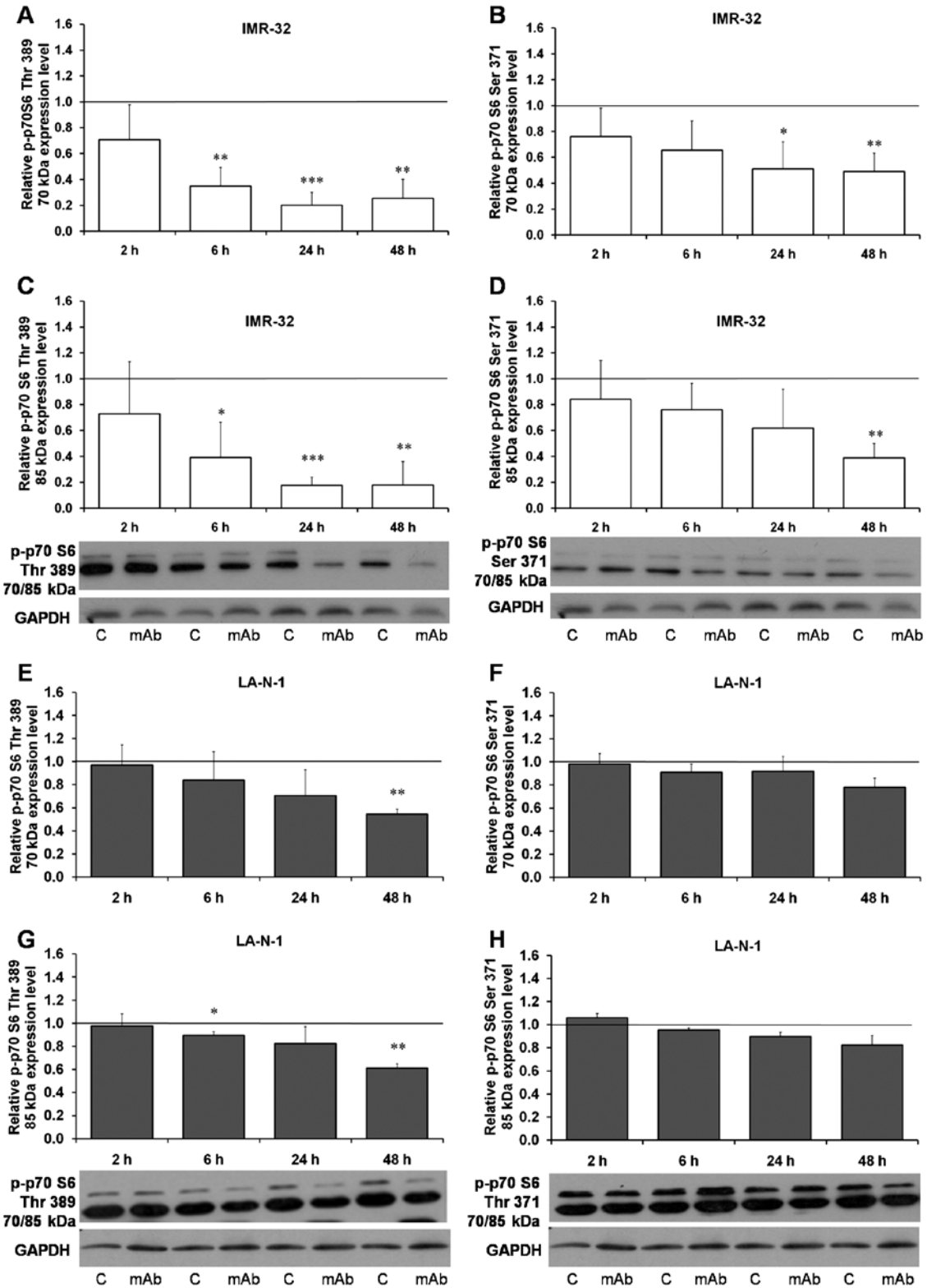

Figure 5. Effect of the 14G2a mAb on p70 S6 phosphorylation. Phosphorylated p70 S6 (p-p70 S6, Thr389 and Ser371) 70 and 85 kDa forms were measured at 2, 6, 24 and 48 h, and normalized to GAPDH. Mean values of three separate experiments obtained for the 14G2a mAb-treated IMR-32 (A-D) and LA-N-1 (E-H) are presented, and calculated versus control values, set as 1 (black baseline). ANOVA shows statistically significant changes of p-p70 S6 Thr389 content in time in the IMR-32 cells for 70 kDa [$F(11,34)$, $p=0.0021$] and 85 kDa isoform [$F(3,9)=5.38$, $p=0.0214$]. ANOVA also shows statistically significant changes of p-p70 S6 Ser371 content in time in the LA-N-1 cells for 85 kDa isoform [$F(3,9)=3.93$, $p=0.0479$]. ANOVA shows no statistically significant changes of expression in time for the rest of the proteins. P-values for t-test were as follows: $^{*}p<0.05$, $^{**}p<0.01$, $^{***}p<0.001$. Below each chart representative immunoblottings are presented: C, control cells; mAb, mAb-treated cells (40 μg/ml).

able for Thr389 phosphorylation (37), was also statistically meaningfully downregulated in the IMR-32 cells (Fig. 5B and D), while in the LA-N-1 cells only insignificant decrease was observed (Fig. 5F and H).

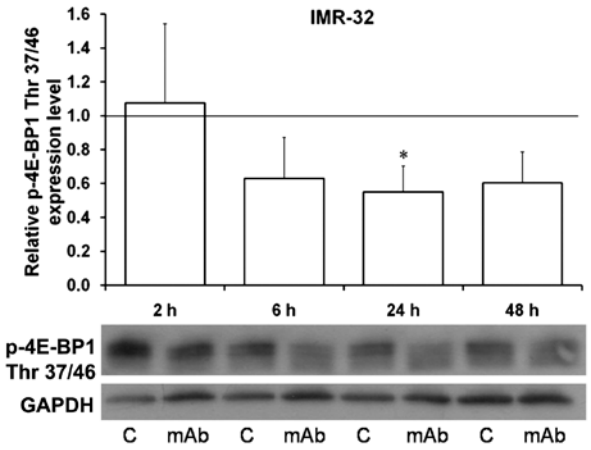

Figure 6. Effect of the 14G2a mAb on 4E-BP1 phosphorylation. Phosphorylated 4E-BP1 (p-4E-BP1, Thr37/46) was measured at 2, 6, 24 and 48 h, and normalized to GAPDH. Mean values of three separate experiments obtained for the 14G2a mAb-treated IMR-32 cells are presented, and calculated versus control values, set as 1 (black baseline). ANOVA shows no statistically significant changes of 4E-BP1 expression in time. P-values for t-test were as follows: $^{*}p<0.05$, $^{**}p<0.01$, $^{***}p<0.001$. Below the chart representative immunoblotting is presented: C, control cells; mAb, mAb-treated cells (40 μg/ml).

4E-BP1 phosphorylation at Thr37/46 by mTORC1 leads to release of its binding protein, eIF-4E, and suppression of inhibition (38,39). The phosphorylated 4E-BP1 was statistically significantly decreased at 24 h in the IMR-32 cells but the decrease was observed already at 6 h (Fig. 6). Dephosphorylation of the protein may indicate that initiation of translation is inhibited. It is not exactly clear how the mTORC1/4E-BP1/eIF4E axis contributes to cancer. It is possible that eIF4E affects cell proliferation and tumorigenesis by promoting the translation of specific mRNAs coding for pro-oncogenic proteins regulating cell survival, cell cycle progression, angiogenesis, energy metabolism and metastasis (15).

AMP-activated protein kinase (AMPK) is inhibited upon the 14G2a mAb treatment. AMPK is one of the principal regulators of mTOR activation and the main energy-saving intracellular enzyme activated by the increased AMP/ATP ratio (40). The AMPK consists of catalytic α and regulatory β and γ subunits (41). The β1 subunit is partially phosphorylated at three sites, Ser24/25, Ser182 and Ser108. The α1 subunit Thr172 is a major, although not exclusive, site of both basal and stimulated phosphorylation by an upstream AMPK kinase. AMPK phosphorylates a number of protein substrates including key enzymes involved in the control of carbohydrate and lipid metabolism, like acetyl-CoA carboxylase (ACC).

Early (at 2 h upon the 14G2a antibody addition) hyperphosphorylation of important amino acid residues (Thr172/Thr174) of the catalytic subunit α of AMPKα1/2 kinase, followed by severe decrease in phosphorylation were observed in the IMR-32 cells (Table I), while decrease in AMPKα isoform protein content was detectable at 2 h (as shown in Fig. 8). Phosphorylation of Ser108 of AMPKβ isoform was statistically significantly decreased in the IMR-32 reaching only 20% of the control level at 48 h (Fig. 7A), while in the CHP-134 it was not changed (Fig. 7D). Thirty-eight and 34 kDa isoforms of the protein were also statistically significantly decreased at 48 h in the IMR-32 cells (Fig. 7B and C), while in CHP-134 the protein level was not changed for the 38 kDa isoform (Fig. 7E) and a significant decrease was found for the 34 kDa isoform only at 48 h (Fig. 7F).

Acetyl coenzyme A carboxylase (ACC) (Fig. 8B) and p-acetyl-ACC (Ser79) (42) (Fig. 8C) were insignificantly decreased at 24 and 48 h, upon an early (2 h) small increase in their content. Kinetics of AMPK-dependent inhibitory phosphorylation of ACC, does not exactly reflect changes in the AMPK itself, which is significantly decreased by the mAb treatment.

PI3K/Akt/mTOR inhibitors modulate effects of the anti-GD2 ganglioside mAb. PI3Ks are lipid kinases that regulate diverse cellular processes including proliferation, adhesion, survival and motility (43). The PI3K signaling pathway frequently becomes dysregulated in human cancers and used by tumor cells for increased proliferation, evasion of apoptosis, tissue invasion and metastasis (44). Therefore PI3Ks have emerged as viable targets for novel anticancer therapy leading to design of potent and selective small molecule inhibitors that have progressed from preclinical tests to even phase III clinical trials (45).

BEZ-235, a novel imidazo-quinoline derivative, is a dual ATP-competitive PI3K and mTOR inhibitor with potent antagonist activity against p110-α, -β, -γ and -δ isoforms and mTOR in nanomolar concentrations (46). The inhibitor drives degradation of MYCN in neuroblastoma tumor cells and decreases angiogenesis (47). Moreover, BEZ235 and the lysosomotropic agent chloroquine synergize to trigger apoptosis in neuroblastoma cells via mitochondrial-lysosomal cross-talk (48). SAR245409 (also known as XL765), another PI3K/mTOR inhibitor, was shown to inhibit proliferation and induce apoptosis in various tumor cell lines (49), in mouse xenograft models (50) and in patients with advanced solid tumors (51,52). Perifosine, a pan-Akt inhibitor of PIP_3 binding, possesses antitumor growth effect alone or in combination with chemotherapy in neuroblastoma (53). Most importantly, perifosine-induced inhibition of Akt increases sensitivity of neuroblastoma to chemotherapy (53). LY294002 is an ATP-competitive PI3K inhibitor which can also directly inhibit mTOR due to structural similarity of mTOR and PI3Ks (12).

Based on the above cited literature, we decided to investigate effects of combinatorial treatment with the 14G2a mAb and the afore-mentioned inhibitors on ATP levels in cultures the three GD2-positive, *MYCN*-amplified neuroblastoma cell lines used in our studies. We show that in IMR-32, CHP-134 and LA-N-1 cells the viability is decreased by all four inhibitors tested alone or in combination with the mAb in a dose-dependent manner after 72 h of treatment (Fig. 9A-L). We calculated and compared IC_{40} values for the inhibitors used alone or in combination with the mAb (Table II). This was based on the results of control experiments with the cell lines treated with the 14G2a mAb alone for 72 h that showed decrease of the cellular ATP levels to 0.47 (±0.01) for IMR-32, 0.46 (±0.02) for CHP-134 and 0.64 (±0.02) for LA-N-1 as compared to the control cells (treated with PBS alone, with $p<0.001$, t-test). The cell lines tested showed variability in sensitivity to the inhibi-

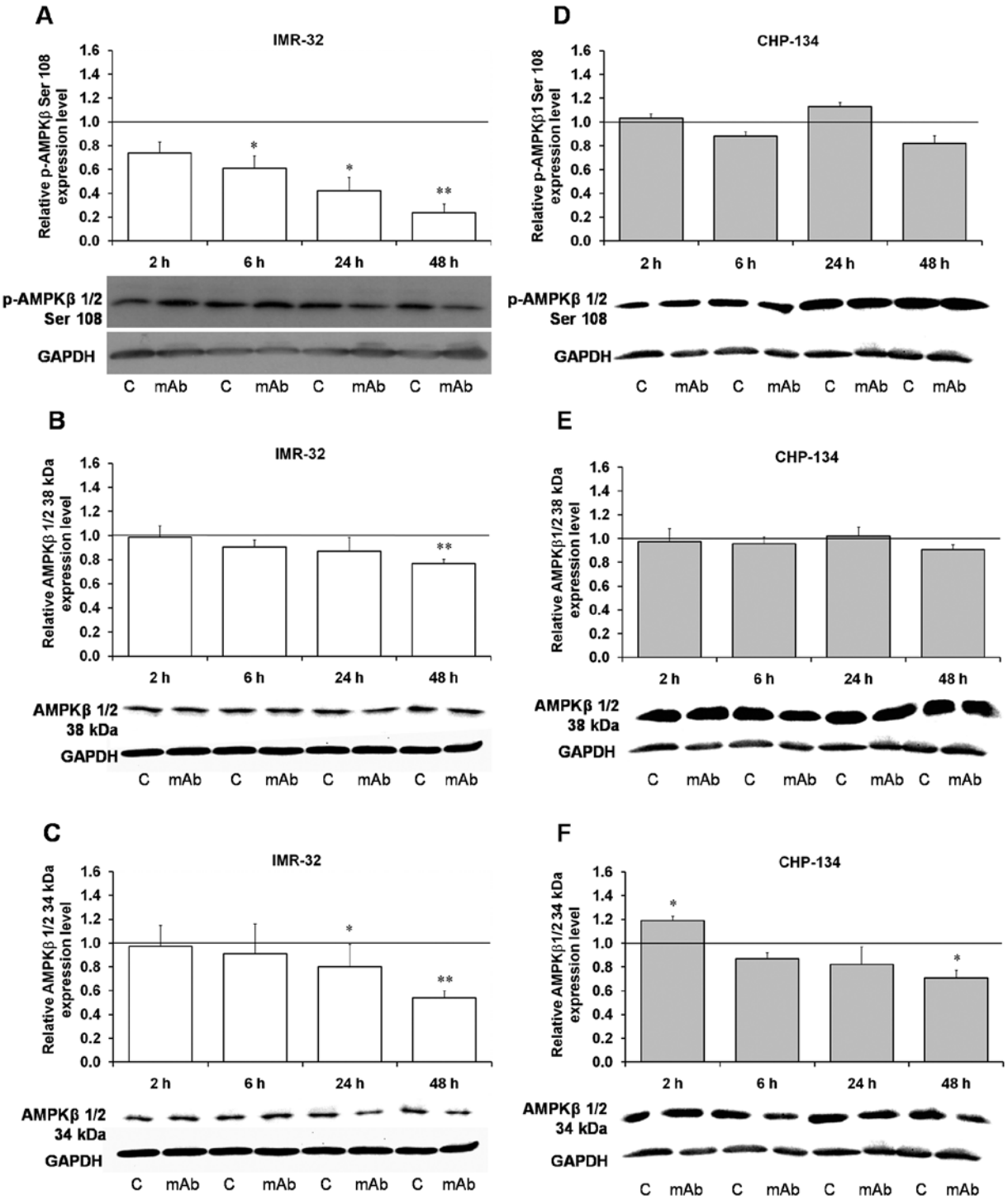

Figure 7. Effect of the 14G2a mAb on AMPKβ expression and phosphorylation. AMPKβ 38 and 34 kDa forms and phosphorylated AMPKβ (p-AMPKβ, Ser108) were measured at 2, 6, 24 and 48 h, and normalized to GAPDH. Mean values of three separate experiments obtained for the 14G2a mAb-treated IMR-32 (A-C) and CHP-134 (D-F) cells are presented for the AMPKβ 38 kDa (B and E), AMPKβ 34 kDa (C and F), and p-AMPKβ (A and D), and calculated versus control values, set as 1 (black baseline). ANOVA shows statistically significant changes of p-AMPKβ Ser108 protein content in time in the IMR-32 cells [$F(3,8)=32.16$, $p=0.0001$] and AMPKβ1/2 34 kDa in the CHP-134 cells [$F(3,9)=5.76$, $p=0.0176$]. ANOVA shows no statistically significant changes of expression in time for the rest of the proteins. P-values for t-test were as follows: $^{*}p<0.05$, $^{**}p<0.01$, $^{***}p<0.001$. Below each chart representative immunoblottings are presented: C, control cells; mAb, mAb-treated cells (40 μg/ml).

tors. BEZ-235 was the most potent, followed by perifosine, LY294002, and SAR245409 (Table II). The observed effects of the dual treatment on ATP contents were inhibitor-dependent and cell line-dependent. The most pronounced changes of IC_{40} values were calculated for combination of the mAb with the LY294002 inhibitor for the CHP-134 cells (17.8-fold change) and the IMR-32 cells (8.4-fold change) as well as for the BEZ-235 inhibitor for the IMR-32 cells (7.2-fold change). For other conditions tested the observed changes in IC_{40} values were rather small, ranging from 1.1 to 2.4. However, we observed that the effects of combinatorial treatment were not always statistically significant as compared to cells treated

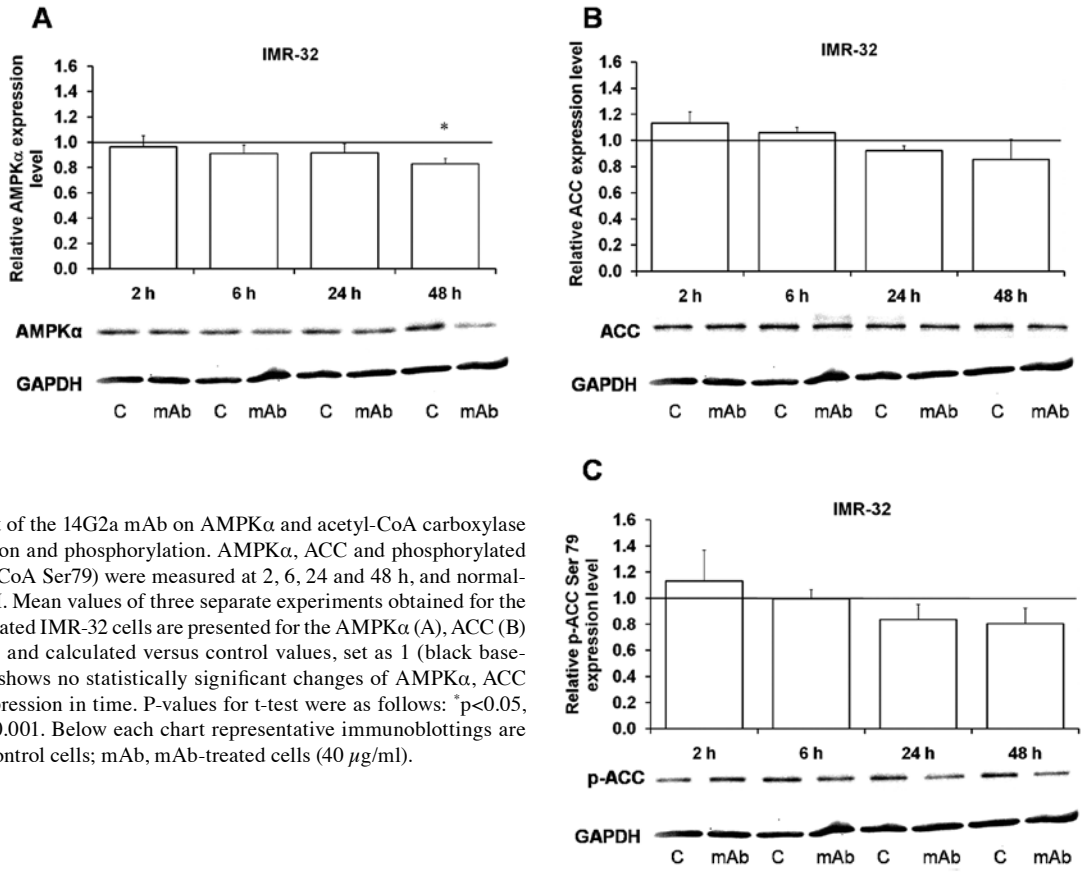

Figure 8. Effect of the 14G2a mAb on AMPKα and acetyl-CoA carboxylase (ACC) expression and phosphorylation. AMPKα, ACC and phosphorylated ACC (p-acetyl CoA Ser79) were measured at 2, 6, 24 and 48 h, and normalized to GAPDH. Mean values of three separate experiments obtained for the 14G2a mAb-treated IMR-32 cells are presented for the AMPKα (A), ACC (B) and p-ACC (C) and calculated versus control values, set as 1 (black baseline). ANOVA shows no statistically significant changes of AMPKα, ACC and p-ACC expression in time. P-values for t-test were as follows: $^{*}p<0.05$, $^{**}p<0.01$, $^{***}p<0.001$. Below each chart representative immunoblottings are presented: C, control cells; mAb, mAb-treated cells (40 μg/ml).

with the inhibitors alone, due to inter-experiment variability that affected calculated values of means and SEMs. This is especially evident for higher doses of the used inhibitors (Fig. 9). In such instances the IC_{40} values should be only used as a trend indication.

Discussion

Constitutive activation of the PI3K/Akt/mTOR signaling network is a frequent event in high-risk neuroblastoma (2,54) and therefore appears to be an attractive therapeutic target. Additionally, the malignancy exhibits increased expression of several growth factor receptors that transmit their signals through the pathway, such as insulin-like growth factor I receptor (IGF-IR), epidermal growth factor receptor (EGFR), tyrosine receptor kinase B (TrkB), platelet-derived growth factor receptor B (PDGFR B), and c-Kit, allowing for selective co-targeting based on mechanism-guided combination that may lead to more effective and durable therapies. Combinatorial treatment of minimal residual disease with the anti-GD2 mAb (ch14.18) and 13-*cis* retinoic acid with addition of IL-2 and GM-CSF has become a standard treatment in high-risk neuroblastoma (5). Based on our previous experimental data showing that the mAb 14G2a causes decrease in viability of IMR-32, LA-N-1 and CHP-134 cells (among other cell lines), we aimed to characterize changes induced with the antibody in the phosphorylation status of several cellular proteins. Our data allowed us to conclude that there are numerous alterations of phosphorylation levels of proteins in the GD2-positive IMR-32 cells treated with the 14G2a mAb. The findings broaden our knowledge on the mechanisms of the antibody actions on the cells and were extended with more thorough analyses of chosen proteins including Akt, PTEN, mTOR, P70 S6, GSK3β, 4E-BP1, AMPK, and P27. We characterized temporal changes of the protein expression levels and their phosphorylation and/or subcellular localization in the mAb-treated cells. Western blot analyses confirmed statistically meaningful decrease in Akt, and mTOR phosphorylation in our models 2-48 h after the 14G2a treatment.

The PI3K/Akt/mTOR and RAS/RAF/MEK/ERK pathways converge to stabilize the expression of the MYC oncoprotein (55). Additionally, it was previously reported that the *MYCN* gene, frequently amplified in neuroblastoma (54), can confer resistance to PI3K/Akt/mTOR inhibitors independently of the RAS pathway (56,12). Also, two PI3K inhibitors, LY294002 and wortmannin, were shown to be able to destabilize MYCN (57). The above literature underlines the significance of inter-connections between the proteins. In this context, our previous studies have shown that MYCN is decreased in the 14G2a mAb-treated, MYCN-amplified IMR-32 and CHP-134 neuroblastoma cells (9). Data reported here allow us to state that the treatment with the 14G2a downregulates not only MYCN, but also mTOR as well as decreases both Akt and mTOR phosphorylation, stressing the ability of the GD2 specific antibody to hit crucial neuroblastoma targets.

It is known that one of the other proteins linked to the PI3K/Akt/mTOR route i.e., GSK-3β, phosphorylates and stabilizes the MYCN protein (58), therefore our result documenting significant decrease in GSK-3β phosphorylation upon the 14G2a mAb addition, is in agreement with our earlier finding

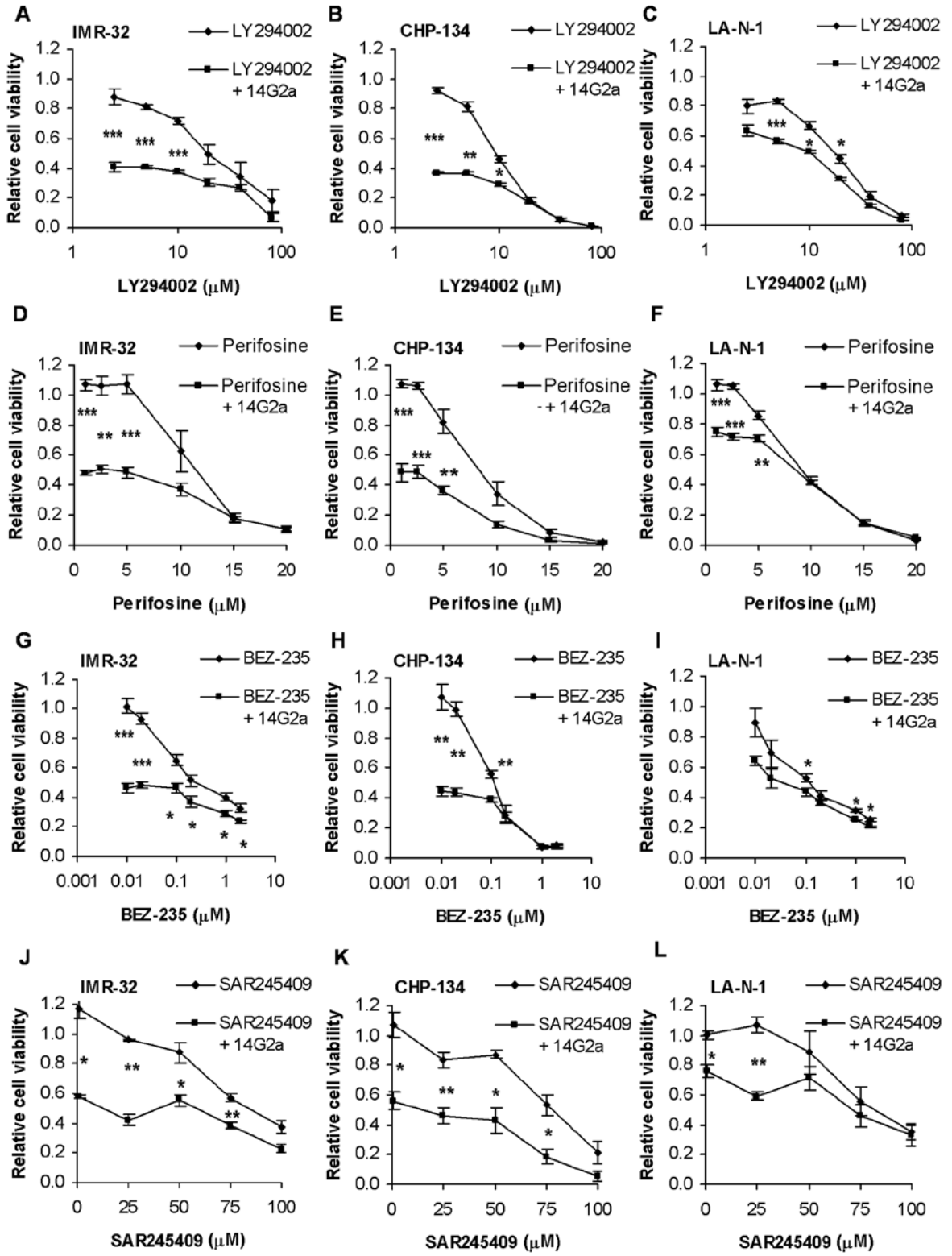

Figure 9. Cell viability measurements. The IMR-32, LA-N-1 and CHP-134 cells were treated with Akt inhibitor (perifosine), dual mTOR/PI3K inhibitors (BEZ-235 and SAR245409), and pan-PI3K inhibitor (LY294002) alone or in combination with the 14G2a mAb (40 μg/ml) for 72 h. The cell viability was determined by measuring ATP content, and compared to respective controls treated with appropriate diluents (DMSO or water, set as 1). Data are presented as means (± SEM) from three (B, C, H and J-L) to four (A, D-G and I) independent experiments (A and B). Logarithmic scales were used for LY294002 and BEZ-235 and linear scales were used for perifosine and SAR245409. P-values for t-test were as follows: $^{*}p<0.05$, $^{**}p<0.01$, $^{***}p<0.001$. The observed effects were shown by ANOVA to be statistically significant for all cell lines treated with either inhibitors alone or combinatorial treatment (data not shown).

on MYCN levels (9). Aurora A kinase is another protein known to stabilize MYCN in human neuroblastoma (59). We have shown before that the 14G2a-induced inhibition of Aurora A kinase accompanied by significant decrease in the MYCN content (9). Other studies have revealed cross-talk of Aurora A kinase with the PI3K pathway at Akt activation (60).

We can support this with our finding showing that Aurora A kinase inhibition with the specific inhibitor MK5108, in the IMR-32 cells resulted in suppression of Akt activation (data not shown).

We wish to highlight that observed inhibition of ERK by the mAb might be important in light of recent findings concerning independent promotion of the accumulation of MYC oncoproteins by ERK and mTOR (54). We have found a decrease in ERK activity in the 14G2a mAb-treated neuroblastoma cells (Table I). Therefore, the kinase may be yet another factor responsible for the observed downregulation of MYCN levels in our model.

We show here that Akt is inhibited in the 14G2a mAb-treated neuroblastoma cell lines, therefore Akt, cannot efficiently phosphorylate and activate MDM2, a negative regulator of P53 and thus cannot inhibit apoptosis. As the P53 and Akt signaling pathways are inter-connected in an opposite manner, therefore inhibition of Akt correlates with upregulation and nuclear accumulation of P53 as observed in our earlier studies (9). Activation of P53 can lead to either cell cycle arrest and DNA repair, or apoptosis (61). We have found decreased phosphorylation of the P53 protein at Ser46, Ser392 and Ser15 in IMR-32 cells (Table I). Phosphorylation of P53 at Ser46 is strongly associated with its proapoptotic activity, therefore decrease in phosphorylation at the amino acid residue could prevent apoptosis. This finding is in agreement with our earlier results, showing that the mAb-induced cell death is only partially caused by apoptosis (8). P53 can be also phosphorylated at Ser15 by different kinases and thus impairs the ability of MDM2 to bind P53, promoting both the accumulation and activation of P53 in response to DNA damage (62). Our results allow us to hypothesize that P53 transcription function can be decreased. On the other hand, dephosphorylation of P53 at Ser392 found in the mAb-treated IMR32 cells, may indicate that P53 is stabilized as phosphorylation of Ser392 is coupled with the rapid turnover of P53 (63).

P27 is a major target of the growth-promoting activity exerted by tyrosine kinase receptors. Moreover, reduced expression of P27 correlates with poor prognosis of patients affected by various types of cancer (29). Akt is responsible for phosphorylation of P27 at Thr157 and Thr198, leading to its cytoplasmic retention and decrease in inhibitory activity against cyclins and Cdks in the nucleus that promotes carcinogenesis (27,28). We observed dephosphorylation of Thr157 and Thr198 of P27 which can be linked with decreased cytoplasmic and increased nuclear accumulation of the cell cycle inhibitor in the IMR-32 cells treated with the 14G2a mAb. We can also conclude that the changes parallel Akt deactivation in our studied model.

The PI3K/Akt/mTOR pathway is dysregulated in cancer and therefore several inhibitors of the route are currently tested in preclinical and clinical settings. The present study shows for the first time, to the best of our knowledge, results of combinatorial treatment of three *MYCN*-amplified neuroblastoma cell lines with the GD2 specific antibody and inhibitors of PI3K/Akt/mTOR pathway. This adds to our previous data on effects of the 14G2a mAb in combination with the Aurora A inhibitor MK-5108 and 13-*cis*-retinoic acid (9). Based on the results, we reckon that PI3K/Akt/mTOR signaling network is inhibited in the 14G2a mAb-treated cells and the antibody can sensitize the cells to the pathway inhibitors to further enhance their antitumor activity, albeit the effects vary depending on the cell line, its sensitivity to the mAb and the small molecule drug used. Among the three PI3K and mTOR inhibitors tested, BEZ-235 was shown to be most potent as the IC_{40} values were lower from 29- to 147-fold as compared to LY294002, from 10- to 65-fold as compared to perifosine, and from 79- to 535-fold when compared to SAR245409 (depending on the cell line treated with each inhibitor). The heterogeneous responses observed advocate for further more detailed studies that may lead to better characterization of the observed effects. This should include more cell lines as well as *in vivo* studies on applicable GD2-mouse neuroblastoma models.

Our understanding of the mechanisms by which GD2-specific antibodies decrease neuroblastoma cell survival is still far from complete. We provide here an explanation of cellular response to the antibody at the level of the PI3K/Akt/mTOR signaling network and other PI3K inter-connected wires. There are numerous elements of the intracellular pathways which are altered upon the mAb addition, including Akt, mTOR and p70 S6 kinases as well as AMPK and PTEN, suppressors of the pathway. Additionally, four different PI3K/Akt/mTOR pathway inhibitors were used in combination with the monoclonal antibody to determine neuroblastoma cell viability. We showed that BEZ-235 was the most potent of the four drugs tested. Effects of combination of the inhibitors with immunotherapy depends on the cell line susceptibility to the given drug and the 14G2a mAb. To conclude, our findings indicate that the 14G2a mAb influences numerous, both disparate and overlapping signal routes. Further studies are warranted in a quest for the best possible combinations of GD2-specific antibodies and other drugs to achieve the greatest anti-proliferative effects on cancer cells.

Acknowledgements

This study was supported by grant no. N301 158635 from the Polish Ministry of Science and Higher Education, NCN-2012/07/B/NZ1/02808 from the Polish National Science Center and DS/8/WBBiB. Faculty of Biochemistry, Biophysics and Biotechnology of the Jagiellonian University is a partner of the Leading National Research Center (KNOW) supported by the Ministry of Science and Higher Education. We thank Dr R.A. Reisfeld (Scripps Institute) for providing us with the hybridoma cell line producing 14G2a mAb. We are grateful to Dr M. Bzowska and Dr J. Skrzeczynska-Moncznik (Immunology Department of the Faculty of Biochemistry, Biophysics and Biotechnology, Jagiellonian University) for help with flow cytometry analyses.

References

1. Modak S and Cheung N-K: Neuroblastoma: Therapeutic strategies for a clinical enigma. Cancer Treat Rev 36: 307-317, 2010.
2. Iżycka-Świeszewska E, Drożyńska E, Rzepko R, Kobierska-Gulida G, Grajkowska W, Perek D and Balcerska A: Analysis of PI3K/AKT/mTOR signalling pathway in high risk neuroblastic tumours. Pol J Pathol 61: 192-198, 2010.
3. Cheung N-KV and Dyer MA: Neuroblastoma: Developmental biology, cancer genomics and immunotherapy. Nat Rev Cancer 13: 397-411, 2013.

4. Hara J: Development of treatment strategies for advanced neuroblastoma. Int J Clin Oncol 17: 196-203, 2012.
5. Yu AL, Gilman AL, Ozkaynak MF, London WB, Kreissman SG, Chen HX, Smith M, Anderson B, Villablanca JG, Matthay KK, *et al*; Children's Oncology Group: Anti-GD2 antibody with GM-CSF, interleukin-2, and isotretinoin for neuroblastoma. N Engl J Med 363: 1324-1334, 2010.
6. Aixinjueluo W, Furukawa K, Zhang Q, Hamamura K, Tokuda N, Yoshida S, Ueda R and Furukawa K: Mechanisms for the apoptosis of small cell lung cancer cells induced by anti-GD2 monoclonal antibodies: Roles of anoikis. J Biol Chem 280: 29828-29836, 2005.
7. Yoshida S, Kawaguchi H, Sato S, Ueda R and Furukawa K: An anti-GD2 monoclonal antibody enhances apoptotic effects of anti-cancer drugs against small cell lung cancer cells via JNK (c-Jun terminal kinase) activation. Jpn J Cancer Res 93: 816-824, 2002.
8. Kowalczyk A, Gil M, Horwacik I, Odrowąż Z, Kozbor D and Rokita H: The GD2-specific 14G2a monoclonal antibody induces apoptosis and enhances cytotoxicity of chemotherapeutic drugs in IMR-32 human neuroblastoma cells. Cancer Lett 281: 171-182, 2009.
9. Horwacik I, Durbas M, Boratyn E, Węgrzyn P and Rokita H: Targeting GD2 ganglioside and Aurora A kinase as a dual strategy leading to cell death in cultures of human neuroblastoma cells. Cancer Lett 341: 248-264, 2013.
10. Cochonneau D, Terme M, Michaud A, Dorvillius M, Gautier N, Frikeche J, Alvarez-Rueda N, Bougras G, Aubry J, Paris F, *et al*: Cell cycle arrest and apoptosis induced by *O*-acetyl-GD2-specific monoclonal antibody 8B6 inhibits tumor growth in vitro and in vivo. Cancer Lett 333: 194-204, 2013.
11. Samuels Y and Ericson K: Oncogenic PI3K and its role in cancer. Curr Opin Oncol 18: 77-82, 2006.
12. Fruman DA and Rommel C: PI3K and cancer: Lessons, challenges and opportunities. Nat Rev Drug Discov 13: 140-156, 2014.
13. Zhang L, Zhou F and ten Dijke P: Signaling interplay between transforming growth factor-β receptor and PI3K/AKT pathways in cancer. Trends Biochem Sci 38: 612-620, 2013.
14. Hers I, Vincent EE and Tavaré JM: Akt signalling in health and disease. Cell Signal 23: 1515-1527, 2011.
15. Laplante M and Sabatini DM: mTOR signaling in growth control and disease. Cell 149: 274-293, 2012.
16. Rodon J, Dienstmann R, Serra V and Tabernero J: Development of PI3K inhibitors: Lessons learned from early clinical trials. Nat Rev Clin Oncol 10: 143-153, 2013.
17. Dienstmann R, Rodon J, Serra V and Tabernero J: Picking the point of inhibition: A comparative review of PI3K/AKT/mTOR pathway inhibitors. Mol Cancer Ther 13: 1021-1031, 2014.
18. Suzuki YJ, Mizuno M and Packer L: Signal transduction for nuclear factor-kappa B activation. Proposed location of antioxidant-inhibitable step. J Immunol 153: 5008-5015, 1994.
19. Niehrs C: The complex world of WNT receptor signalling. Nat Rev Mol Cell Biol 13: 767-779, 2012.
20. Koul HK, Pal M and Koul S: Role of p38 MAP kinase signal transduction in solid tumors. Genes Cancer 4: 342-359, 2013.
21. Liu Y, Gorospe M, Yang C and Holbrook NJ: Role of mitogen-activated protein kinase phosphatase during the cellular response to genotoxic stress. Inhibition of c-Jun N-terminal kinase activity and AP-1-dependent gene activation. J Biol Chem 270: 8377-8380, 1995.
22. Davison K, Mann KK, Waxman S and Miller WH Jr: JNK activation is a mediator of arsenic trioxide-induced apoptosis in acute promyelocytic leukemia cells. Blood 103: 3496-3502, 2004.
23. Cuadrado A and Nebreda AR: Mechanisms and functions of p38 MAPK signalling. Biochem J 429: 403-417, 2010.
24. Walsh MF, Thamilselvan V, Grotelueschen R, Farhana L and Basson M: Absence of adhesion triggers differential FAK and SAPKp38 signals in SW620 human colon cancer cells that may inhibit adhesiveness and lead to cell death. Cell Physiol Biochem 13: 135-146, 2003.
25. Darnell JE Jr, Kerr IM and Stark GR: Jak-STAT pathways and transcriptional activation in response to IFNs and other extracellular signaling proteins. Science 264: 1415-1421, 1994.
26. Beierle EA, Ma X, Stewart J, Nyberg C, Trujillo A, Cance WG and Golubovskaya VM: Inhibition of focal adhesion kinase decreases tumor growth in human neuroblastoma. Cell Cycle 9: 1005-1015, 2010.
27. Motti ML, De Marco C, Califano D, Fusco A and Viglietto G: Akt-dependent T198 phosphorylation of cyclin-dependent kinase inhibitor p27kip1 in breast cancer. Cell Cycle 3: 1074-1080, 2004.
28. Viglietto G, Motti ML and Fusco A: Understanding p27(kip1) deregulation in cancer: Down-regulation or mislocalization. Cell Cycle 1: 394-400, 2002.
29. Pourmand G, Ziaee AA, Abedi AR, Mehrsai A, Alavi HA, Ahmadi A and Saadati HR: Role of PTEN gene in progression of prostate cancer. Urol J 4: 95-100, 2007.
30. Guertin DA, Stevens DM, Saitoh M, Kinkel S, Crosby K, Sheen JH, Mullholland DJ, Magnuson MA, Wu H and Sabatini DM: mTOR complex 2 is required for the development of prostate cancer induced by Pten loss in mice. Cancer Cell 15: 148-159, 2009.
31. Yang Z, Yuan XG, Chen J, Luo SW, Luo ZJ and Lu NH: Reduced expression of PTEN and increased PTEN phosphorylation at residue Ser380 in gastric cancer tissues: A novel mechanism of PTEN inactivation. Clin Res Hepatol Gastroenterol 37: 72-79, 2013.
32. Robertson BW, Bonsal L and Chellaiah MA: Regulation of Erk1/2 activation by osteopontin in PC3 human prostate cancer cells. Mol Cancer 9: 260, 2010.
33. Chiang GG and Abraham RT: Phosphorylation of mammalian target of rapamycin (mTOR) at Ser-2448 is mediated by p70S6 kinase. J Biol Chem 280: 25485-25490, 2005.
34. Hong S, Zhao B, Lombard DB, Fingar DC and Inoki K: Cross-talk between sirtuin and mammalian target of rapamycin complex 1 (mTORC1) signaling in the regulation of S6 kinase 1 (S6K1) phosphorylation. J Biol Chem 289: 13132-13141, 2014.
35. Dufner A and Thomas G: Ribosomal S6 kinase signaling and the control of translation. Exp Cell Res 253: 100-109, 1999.
36. Pullen N and Thomas G: The modular phosphorylation and activation of p70s6k. FEBS Lett 410: 78-82, 1997.
37. Pearson RB, Dennis PB, Han JW, Williamson NA, Kozma SC, Wettenhall RE and Thomas G: The principal target of rapamycin-induced p70s6k inactivation is a novel phosphorylation site within a conserved hydrophobic domain. EMBO J 14: 5279-5287, 1995.
38. Dowling RJ, Topisirovic I, Alain T, Bidinosti M, Fonseca BD, Petroulakis E, Wang X, Larsson O, Selvaraj A, Liu Y, *et al*: mTORC1-mediated cell proliferation, but not cell growth, controlled by the 4E-BPs. Science 328: 1172-1176, 2010.
39. Sonenberg N and Hinnebusch AG: Regulation of translation initiation in eukaryotes: Mechanisms and biological targets. Cell 136: 731-745, 2009.
40. Kahn BB, Alquier T, Carling D and Hardie DG: AMP-activated protein kinase: Ancient energy gauge provides clues to modern understanding of metabolism. Cell Metab 1: 15-25, 2005.
41. Mitchelhill KI, Michell BJ, House CM, Stapleton D, Dyck J, Gamble J, Ullrich C, Witters LA and Kemp BE: Posttranslational modifications of the 5'-AMP-activated protein kinase β1 subunit. J Biol Chem 272: 24475-24479, 1997.
42. Ha J, Daniel S, Broyles SS and Kim KH: Critical phosphorylation sites for acetyl-CoA carboxylase activity. J Biol Chem 269: 22162-22168, 1994.
43. Cantley LC: The phosphoinositide 3-kinase pathway. Science 296: 1655-1657, 2002.
44. Osaki M, Oshimura M and Ito H: PI3K-Akt pathway: Its functions and alterations in human cancer. Apoptosis 9: 667-676, 2004.
45. Akinleye A, Avvaru P, Furqan M, Song Y and Liu D: Phosphatidylinositol 3-kinase (PI3K) inhibitors as cancer therapeutics. J Hematol Oncol 6: 88, 2013.
46. Maira SM, Stauffer F, Brueggen J, Furet P, Schnell C, Fritsch C, Brachmann S, Chène P, De Pover A, Schoemaker K, *et al*: Identification and characterization of NVP-BEZ235, a new orally available dual phosphatidylinositol 3-kinase/mammalian target of rapamycin inhibitor with potent in vivo antitumor activity. Mol Cancer Ther 7: 1851-1863, 2008.
47. Chanthery YH, Gustafson WC, Itsara M, Persson A, Hackett CS, Grimmer M, Charron E, Yakovenko S, Kim G, Matthay KK, *et al*: Paracrine signaling through MYCN enhances tumor-vascular interactions in neuroblastoma. Sci Transl Med 4: 115ra3, 2012.
48. Seitz C, Hugle M, Cristofanon S, Tchoghandjian A and Fulda S: The dual PI3K/mTOR inhibitor NVP-BEZ235 and chloroquine synergize to trigger apoptosis via mitochondrial-lysosomal cross-talk. Int J Cancer 132: 2682-2693, 2013.
49. Garcia-Echeverria C and Sellers WR: Drug discovery approaches targeting the PI3K/Akt pathway in cancer. Oncogene 27: 5511-5526, 2008.
50. Yu P, Laird AD, Du X, Wu J, Won KA, Yamaguchi K, Hsu PP, Qian F, Jaeger CT, Zhang W, *et al*: Characterization of the activity of the PI3K/mTOR inhibitor XL765 (SAR245409) in tumor models with diverse genetic alterations impacting the PI3K pathway. Mol Cancer Ther 13: 1078-1091, 2014.

51. Papadopoulos KP, Tabernero J, Markman B, Patnaik A, Tolcher AW, Baselga J, Shi W, Egile C, Ruiz-Soto R, Laird AD, *et al*: Phase I safety, pharmacokinetic, and pharmacodynamic study of SAR245409 (XL765), a novel, orally administered PI3K/mTOR inhibitor in patients with advanced solid tumors. Clin Cancer Res 20: 2445-2456, 2014.
52. Jänne PA, Cohen RB, Laird AD, Macé S, Engelman JA, Ruiz-Soto R, Rockich K, Xu J, Shapiro GI, Martinez P, *et al*: Phase I safety and pharmacokinetic study of the PI3K/mTOR inhibitor SAR245409 (XL765) in combination with erlotinib in patients with advanced solid tumors. J Thorac Oncol 9: 316-323, 2014.
53. Li Z, Yan S, Attayan N, Ramalingam S and Thiele CJ: Combination of an allosteric Akt Inhibitor MK-2206 with etoposide or rapamycin enhances the antitumor growth effect in neuroblastoma. Clin Cancer Res 18: 3603-3615, 2012.
54. Johnsen JI, Segerström L, Orrego A, Elfman L, Henriksson M, Kågedal B, Eksborg S, Sveinbjörnsson B and Kogner P: Inhibitors of mammalian target of rapamycin downregulate MYCN protein expression and inhibit neuroblastoma growth in vitro and in vivo. Oncogene 27: 2910-2922, 2008.
55. Lee T, Yao G, Nevins J and You L: Sensing and integration of Erk and PI3K signals by Myc. PLOS Comput Biol 4: e1000013, 2008.
56. Maris JM, Hogarty MD, Bagatell R and Cohn SL: Neuroblastoma. Lancet 369: 2106-2120, 2007.
57. Chesler L, Schlieve C, Goldenberg DD, Kenney A, Kim G, McMillan A, Matthay KK, Rowitch D and Weiss WA: Inhibition of phosphatidylinositol 3-kinase destabilizes Mycn protein and blocks malignant progression in neuroblastoma. Cancer Res 66: 8139-8146, 2006.
58. Duffy DJ, Krstic A, Schwarzl T, Higgins DG and Kolch W: GSK3 inhibitors regulate MYCN mRNA levels and reduce neuroblastoma cell viability through multiple mechanisms, including p53 and Wnt signaling. Mol Cancer Ther 13: 454-467, 2014.
59. Otto T, Horn S, Brockmann M, Eilers U, Schüttrumpf L, Popov N, Kenney AM, Schulte JH, Beijersbergen R, Christiansen H, *et al*: Stabilization of N-Myc is a critical function of Aurora A in human neuroblastoma. Cancer Cell 15: 67-78, 2009.
60. Yao JE, Yan M, Guan Z, Pan CB, Xia LP, Li CX, Wang LH, Long ZJ, Zhao Y, Li MW, *et al*: Aurora-A down-regulates IkappaBalpha via Akt activation and interacts with insulin-like growth factor-1 induced phosphatidylinositol 3-kinase pathway for cancer cell survival. Mol Cancer 8: 95, 2009.
61. Levine AJ: p53, the cellular gatekeeper for growth and division. Cell 88: 323-331, 1997.
62. Loughery J, Cox M, Smith LM and Meek DW: Critical role for p53-serine 15 phosphorylation in stimulating transactivation at p53-responsive promoters. Nucleic Acids Res 42: 7666-7680, 2014.
63. Cox ML and Meek DW: Phosphorylation of serine 392 in p53 is a common and integral event during p53 induction by diverse stimuli. Cell Signal 22: 564-571, 2010.